NASA TECHNICAL NOTE

NASA TN D-4137

NASA TN D-4137

DETERMINATION OF TUNGSTEN RESONANCE ABSORPTION INTEGRALS BY ACTIVATION

by Clarence R. Pierce and Donald F. Shook

Lewis Research Center
Cleveland, Ohio

NATIONAL AERONAUTICS AND SPACE ADMINISTRATION • WASHINGTON, D. C. • OCTOBER 1967

NASA TN D-4137

DETERMINATION OF TUNGSTEN RESONANCE ABSORPTION INTEGRALS BY ACTIVATION

By Clarence R. Pierce and Donald F. Shook

Lewis Research Center
Cleveland, Ohio

NATIONAL AERONAUTICS AND SPACE ADMINISTRATION

For sale by the Clearinghouse for Federal Scientific and Technical Information
Springfield, Virginia 22151 – CFSTI price $3.00

DETERMINATION OF TUNGSTEN RESONANCE ABSORPTION INTEGRALS BY ACTIVATION

by Clarence R. Pierce and Donald F. Shook

Lewis Research Center

SUMMARY

The effective resonance integrals of tungsten 186 and tungsten 184 as contained in natural tungsten were obtained for foil thicknesses from 0.25 to about 10^{-7} centimeter. Thin-sample activations yielded values for the dilute resonance integrals of 443±17 barns ($(4.43\pm0.17)10^{-26}$ m^2) for W^{186} and 15±2 barns ((1.5 ± 0.2) 10^{-27} m^2) for W^{184}.

Since the 18.8-electron-volt (3.01×10^{-18} J) resonance of W^{186} constitutes 92 percent of the dilute resonance integral for this isotope, and since the neutron scattering width for this resonance has been accurately measured, the present measurement provides an estimate of the radiative capture width. The scattering widths for the important resonances of W^{184} are also accurately known, and therefore an average capture width for this isotope was also estimated. Values of 0.041±0.002 electron volt ((6.56 ± 0.32) 10^{-21} J) for the capture width of the 18.8-electron-volt (3.01×10^{-18} J) resonance of W^{186} and 0.062±0.007 electron volt ((9.93 ± 1.12) 10^{-21} J) for the capture widths of the main resonances of W^{184} were obtained. The capture width obtained for the 18.8-electron-volt (3.01×10^{-18} J) resonance of W^{186} is lower than but in agreement with the reported neutron spectroscopy result of 0.045±0.006 electron volt ((7.21 ± 0.96) 10^{-21} J).

In the thick-sample region, computed values of the resonance integrals for W^{186} obtained by the Nordheim integral method significantly overestimate experimental values. This result is ascribed to resonance overlap between W^{182} and W^{186} which is of importance in the natural tungsten samples used. In addition, the flat source approximation used in the calculation reduces the precision of the calculation for materials with highly scattering resonances, such as W^{186}.

In addition to the resonance integral measurements, a determination of 76.4±0.7 days was made for the half-life of W^{185}, compared with published values ranging from 73.2±0.5 to 76.2±0.4 days.

INTRODUCTION

The potential value of tungsten in high-temperature nuclear reactors has generated considerable interest in the nuclear parameters of the tungsten isotopes (ref. 1). The epicadmium effective resonance absorption integrals of the tungsten 186 and tungsten 184 isotopes are considered herein.

Two experimental techniques, the reactivity method and the activation method, are used to determine resonance integrals. The reactivity method determines the capture rate of a sample from the reactivity caused by insertion of the sample into a reactor. This method has been used to determine effective resonance integrals for natural tungsten and for the isotopes of tungsten relative to gold as a standard (refs. 2 and 3). The reactivity method is limited to sizes of samples that produce measurable changes in reactivity. A major limitation of the reactivity method as applied to W^{184} lies in the relatively large absorptivities of the residual tungsten isotopes in highly enriched samples of W^{184}. Thus, the measured reactivity is for a mixed sample, and the W^{184} resonance integral must be deduced from measurements on samples each enriched in a different isotope of tungsten. The activation method overcomes this problem since W^{184} capture rates can be measured directly by determining W^{185} activities. The activation method is limited to W^{184} and W^{186} since neutron capture by W^{182} and W^{183} yields stable nuclides. The rare isotope W^{180} also activates but is not considered herein because of its limited natural abundance (0.14 percent).

Computer codes are available for calculating resonance integrals from resonance parameters. For the general case of finite-sized samples with resonance self-shielding, the Nordheim integral treatment (refs. 4 and 5) has been used to calculate effective resonance integrals. Samples with various surface to mass ratios S/M ranging from thick to infinitely dilute have been computed. The code had been used previously to compute resonance integrals for uranium 238 and resulted in good agreement with experiment. An epicadmium 1/v component must be added to the calculated resonance integral for comparison with measured values. For the unresolved energy region, where the resonance parameters are unknown, a separate routine that uses statistical parameters computes average s-wave cross sections; average p-wave and higher l-wave contributions must be computed separately.

In the calculations, a flat source of scattered neutrons is assumed to exist in the sample. Cohen (ref. 6) evaluated this assumption by allowing a shaped source within the sample. For the strongly scattering 18.8-electron-volt (3.01×10^{-18} J) resonance of W^{186}, significantly lower capture integrals were calculated for thick samples by Cohen, using more reasonable source distributions. In addition, there is cross-section overlap in the common wings of the resonances at 18.8 electron volts (3.01×10^{-18} J) in W^{186} and at 21.2 electron volts (3.39×10^{-18} J), in W^{182}. Westfall (ref. 7) investigated the effect of this overlap in natural tungsten.

METHOD AND ANALYSIS

The infinitely dilute resonance capture integral for an isotope x is defined by

$$I_\infty = \int_{E_{Cd}}^{\infty} \sigma_a^x(E) \frac{dE}{E} \tag{1}$$

where E is the neutron energy, E_{Cd} is the lower energy limit, and $\sigma_a^x(E)$ is the neutron capture cross section of isotope x. (All symbols are defined in appendix A.) The lower energy limit is standardized here to 0.5 electron volt (8.0×10^{-20} J).

Dilute resonance integrals were measured by the activation method that employs cadmium shields. The method consists of measuring cadmium-shielded-sample and bare-sample activities that result from exposure to a thermal reactor flux. These activities are compared with the cadmium-shielded and bare activities of a material that has an accurately known resonance integral and thermal cross section.

The cadmium ratio R^x for an isotope x exposed to a given flux is defined as

$$R^x = \frac{B^x/\epsilon_b}{C^x/\epsilon_c} \tag{2}$$

where C is the saturated count rate for the cadmium-shielded sample, B is the saturated count rate for the bare sample, and ϵ_c and ϵ_b are the respective counting efficiencies. Therefore, R^x is equal to the capture rate ratio.

Unknown resonance integrals can be determined relative to a known standard by using the following relation (ref. 8):

$$I_\infty^x = \frac{R^s - 1}{R^x - 1} \frac{\sigma_{th}^x}{\sigma_{th}^s} I_\infty^s \tag{3}$$

where I_∞ is the infinitely dilute resonance integral, R is the cadmium ratio, σ_{th} is the microscopic absorption cross section at 0.025 electron volt (4.00×10^{-21} J). The superscripts s and x represent the standard sample and the isotope under investigation, respectively. Equation (3) arises simply by expressing the capture rates as proportional to the resonance integral and to the thermal cross section plus the resonance integral. The following assumptions are therefore implicit in equation (3):

(1) The neutron flux varies as 1/E above the cadmium cutoff energy.

(2) Both the bare and the cadmium-shielded samples are exposed to the same flux

above a cadmium cutoff energy.

(3) The cadmium absorbs all the neutrons below the cadmium cutoff energy; that is, the assumption of a flux discontinuity is invoked at the cutoff energy.

(4) The sample absorption cross sections below the cutoff energy must have the same energy variation as the standard. This assumption is good for the isotopes measured in this experiment (ref. 9).

Since some of the conditions listed may not be satisfied, their effect on the results of the measurements were investigated. Some knowledge of the flux energy dependence within the reactor core is necessary for such a study. Figure 1 represents the calculated reactor flux with and without the cadmium shield as used in the present experiment. These values were obtained by using a one-dimensional transport code developed in this laboratory (ref. 10) which makes use of the energy group structure of GAM II (ref. 11). The fluxes were normalized to a value of 1 at 4.9 electron volts (7.85×10^{-19} J). The calculation shows a deviation of the flux from a 1/E variation and an absence of the required discontinuity at 0.5 electron volt (8.0×10^{-20} J).

A calculated correction to the experiment is used to account for the deviation of the flux from that required in equation (3). The method used to obtain the correction is treated in detail in appendix B. The resulting formula is

$$I_{eff}^{x} = \frac{(R^{Au} - 1)}{(R^{x} - 1)} \frac{\left(\sigma_{th}^{x}\right)_{eff}}{\left(\sigma_{th}^{Au}\right)_{eff}} I_{eff}^{Au} \mu \tag{4}$$

where I_{eff} is the effective resonance integral, $(\sigma_{th})_{eff}$ is the effective thermal capture cross section, and μ is the calculated correction factor. The factor μ is evaluated in appendix B and is 0.955 for W^{186} and 0.886 for W^{184} for the case of thin or dilute samples. Equation (4) yields an I_{eff}^{x} referred to a cadmium cutoff of 0.5 electron volt (8.0×10^{-20} J). The correction μ is based on the fluxes shown in figure 1 and does not include a possible effect of the observed overlap of a cadmium and a tungsten resonance at 18.5 electron volts (2.96×10^{-18} J). This effect is accounted for herein by using detailed cross sections for these resonances.

Resonance parameters for the 18.5-electron-volt (2.96×10^{-18} J) resonance in cadmium 113 are reported in reference 12. These are $\Gamma_n = (2.8\pm0.2)10^{-4}$ electron volt ($(4.48\pm0.32)10^{-23}$ J), and $\Gamma_\gamma = 0.115$ electron volt (1.84×10^{-20} J). The statistical weight factor for this resonance is 0.75. Figure 2 shows the Doppler broadened neutron capture cross sections for the cadmium 113 resonance plotted with the Doppler broadened neutron capture cross sections for the 18.8-electron-volt (3.01×10^{-18} J) resonance in W^{186}. The W^{186} parameters used were $\Gamma_n = 0.319$ electron volt (5.11×10^{-20} J) and

Γ_γ = 0.044 electron volt (7.05×10^{-21} J). The computer program that was used for calculating resonance integrals (ref. 5) was also used to generate the cross sections. The cadmium 113 cross sections were used to determine the transmission of the cadmium over the energy range from 18.2 to 18.8 electron volts (2.91×10^{-18} to 3.01×10^{-18} J). The product of macroscopic cross section and thickness $\Sigma_a(E)\tau$ varies as 4.98×10^{-4} $\sigma_a(E)$ for the 0.089-centimeter-thick cadmium, which has a density of 8.6 grams per cubic centimeter and a cadmium 113 natural abundance of 12.26 percent. The total transmission probability T(E) for the cadmium shield and a given neutron energy is obtained from the following formula:

$$T = 2\int_0^{\pi/2} \cos\theta e^{-\Sigma_a\tau/\cos\theta} \sin\theta\, d\theta$$

$$= 2E_3(\Sigma_a\tau) \tag{5}$$

Values for $E_3(\Sigma_a\tau)$ were obtained from tabulated values in reference 13. To obtain the energy integral values, the quantities $\sigma_a^{W^{186}}\ \Delta E/E$ and $T\sigma_a^{W^{186}}\ \Delta E/E$ were integrated by using the trapezoidal rule. Table I summarizes the values obtained from these calculations. For the cadmium 113 resonance at 18.5 electron volts (2.96×10^{-18} J), the cadmium shielding results in a 2-percent reduction in the infinitely dilute W^{186} resonance integral. If an appreciable energy uncertainty is assumed so that the cadmium 113 resonance is actually located at 18.8 electron volts (3.01×10^{-18} J) there is a 3-percent reduction in the W^{186} resonance integral.

EXPERIMENT

Three experimental techniques were used to obtain resonance integrals for W^{186} and W^{184}. In the first technique, cadmium ratios of extremely thin foils were measured to determine the dilute resonance integrals of both W^{186} and W^{184}. In the second technique, relative W^{187} activities for a range of foil thicknesses were determined, and the data were normalized to the dilute resonance integral of W^{186}. Relative gold 198 (Au^{198}) activities were also determined and normalized to the dilute resonance integral of Au^{197}. The third technique consisted of determining a thick-sample cadmium ratio to obtain an effective resonance integral for W^{184}.

Activation Procedure

Bare and cadmium-shielded samples were irradiated in the center of the NASA Zero

Power Reactor-1 (ZPR-1). ZPR-1 is a uranyl fluoride - water solution reactor. Criticality is achieved by increasing the solution height in a 30.5-centimeter-diameter tank. The UO_2F_2 concentration, about 7 weight percent for this experiment, determines the solution height at which the system goes critical. The critical height is measured by a platinum wire probe. During the time of the measurements, the clean core critical height was 43 to 45.5 centimeters and the height with cadmium was 45.3 to 47.8 centimeters. Figure 3 is a cutaway drawing of the reactor vessel and shows a foil holder suspended in the solution. The foils are positioned in the core center by adjusting the height of the foil holder with small screws (not shown) at the supporting bracket at the top of the reactor tank. The samples are placed in the O-ring-sealed Lucite holder to isolate them from the reactor fuel solution. Gold monitor foils used to correct for power variation were positioned on the outside of the tank.

A high level of activity was required to investigate the relation between the bare and cadmium-covered counting efficiencies ϵ_b and ϵ_c; therefore, natural tungsten foils were irradiated in the Plum Brook reactor at Sandusky, Ohio (ref. 14). The irradiations were carried out in the hydraulic rabbit facility RA-8 in the water reflector.

Sample Preparation

A series of samples vacuum deposited on 0.00254-centimeter-thick high-purity aluminum was prepared. The thinnest sample was prepared by using metallic tungsten. This method requires a high filament temperature and a long time to build up a sufficiently thick deposit. The chance of sample contamination from the electrodes and from breakdown of diffusion pump oil is high. Therefore, all but the thinnest of this series of samples was obtained by depositing a salt containing tungsten. A disadvantage of this method is that the mass of tungsten cannot be directly determined, since the chemical composition of the deposit is not well known. This knowledge is not important with the cadmium ratio method when the same thin sample is used for both the bare and the cadmium-covered irradiations.

The salt was prepared by dissolving high-purity tungsten metal in an aqueous solution of nitric acid (HNO_3) and hydrofluoric acid (HF). The tungsten oxide (WO_3) resulting from this process was dissolved in a sodium hydroxide solution which yielded an alkaline solution of sodium tungstate (Na_2WO_4). Drying produced the dihydrate, $Na_2WO_4 \cdot 2H_2O$. The sodium tungstate was deposited from a platinum boat with a perforated platinum cover at a pressure of 10^{-5} to 10^{-4} millimeters of mercury (1.3×10^{-3} to 1.3×10^{-2} N/m^2). X-ray spectroscopic examination of a sample indicated that the deposit was sodium tungstate, with some indication of tungstic acid.

Gold metal samples were prepared by vacuum deposition from tungsten wire baskets on to 0.00254-centimeter-thick aluminum. In addition, two samples were made by first vacuum depositing gold on 0.00254-centimeter-thick aluminum and then vacuum depositing Na_2WO_4 on the gold. The tungsten salt on one of these samples was prepared from tungsten enriched to 84.7 percent in tungsten 186.

The weights of the deposits were determined by weighing the aluminum before and after deposition. In general, all weights were obtained to within 50 percent, with better accuracy for heavier samples. Values of surface-area to mass ratio were computed from the weights and compositions of the deposits. Since the variation of I_{eff} with sample size is small in this region, errors in S/M are not important.

Additional thin films were made by electroplating natural tungsten on 0.08-centimeter-thick aluminum. These samples were supplied by Oak Ridge National Laboratories (ORNL) and were approximately 22.5 square centimeters in area. The tungsten mass was determined after counting data were taken by removing the tungsten and spectrophotometrically determining the amount. The mass measurement was done at ORNL, and the activation and counting were done at Lewis. For thicker samples, foils were cut from high-purity tungsten and gold sheets, 0.0127, 0.0076, and 0.0025 centimeter thick.

Counting Method

Both β-ray and γ-ray counting techniques were used in the measurements. All gamma counting was done by using a thallium-activated sodium iodide (NaI(Tl)) crystal 7.62 centimeters in diameter by 7.62 centimeters thick, with a 0.56-centimeter-thick aluminum β-ray absorber. The samples were positioned 3.17 centimeters above the center of the flat face of the crystal. Energy calibration of the single-channel analyzer was checked using Au^{198} and cesium 137. The window of the analyzer was set to encompass the desired energy range, which in most cases was 0.3 to 0.8 MeV (4.8×10^{-13} to 12.8×10^{-13} J).

An intense γ-ray of 0.41 MeV (5.25×10^{-13} J) is emitted by Au^{198}. One of much lower intensity is located at 0.68 MeV (8.71×10^{-13} J). A large number of γ-rays are emitted by W^{187}; the principal ones are of 0.686- and 0.552-MeV (8.79×10^{-13} and 7.07×10^{-13} J) energy. When both Au^{198} and W^{187} were present in a sample, the window was adjusted to cover just the 0.41-MeV (5.25×10^{-13} J) peak of Au^{198}, and adjusted separately to include just the 0.686-MeV (8.79×10^{-13} J) peak in the γ-ray spectrum of W^{187}. This facilitated separating the respective count rates. A 400-channel analyzer was also used to check on the purity of the samples.

In the case of W^{185}, only one γ-ray is released in 0.018 percent of the decays (ref. 16). This γ-ray of 0.125 MeV (1.602×10^{-13} J) is emitted along with γ-rays of

0.136 and 0.153 MeV (2.18×10^{-13} J and 2.45×10^{-13} J) from W^{181}. The complexity and the low energy and intensity of this γ-ray spectrum made it advisable to determine the W^{184} activation by beta counting, which is discussed later in this section.

Count-rate data as a function of time for all samples were plotted on semilog paper. Since many samples consisted of more than one radioactive isotope, the counting rate of each isotope had to be obtained. The half-lives of W^{187} and W^{185} are dissimilar enough to permit waiting for the W^{187} to decay to a negligible value. End-of-irradiation count-rate values were obtained by standard formula from count rates taken on different days, and an average value was obtained from these values. This method also yielded the standard deviation of the data. Tungsten 187 beta count rates were obtained by taking the difference between the W^{185} and the total count rates for the sample. When both Au^{198} and W^{187} were present in the sample, it was necessary to obtain the isotopic count rates from pairs of count-rate values taken on different days.

A half-life of 24.0 hours was used for extrapolating count rates to the end-of-irradiation values for W^{187}. For W^{185}, extensive counting periods were obtained from the samples irradiated in the Plum Brook reactor. Several dried deposit samples made from these samples had enough beta activity to permit counting with good statistics over a period of several half-lives (approximately 12 months for one of the samples). Tungsten 181 γ- and x-ray emissions from these sodium tungstate deposits were small since the samples represented only a small fraction of the original foil and since the beta-counting efficiency was much greater than for the original foil. Tungsten 185 was used to determine the counter plateau, and checks were made on the counter plateau by monitoring with a depleted uranium sample. These observations yield a half-life of 76.4±0.7 days. This value was used to extrapolate the W^{185} data back to end-of-irradiation values. Previous measurements list values ranging from 73.2±0.5 to 75.1±0.6 days (ref. 15, p. B1-1-90), and 76.2±0.4 days (ref. 16).

The electroplated films were irradiated with an 0.08-centimeter-thick aluminum blank of the same diameter as the film backing. This method permitted subtraction of the gamma background from the aluminum backing of the electroplated film samples. Activation of the manganese impurity in the thick aluminum backing necessitated waiting a day before the tungsten activity became significant.

Stacks of 0.0127-centimeter-thick samples were irradiated for activation of thick tungsten samples. The 0.0127-centimeter-thick samples that made up the stack were gamma counted separately and their sum was obtained. This procedure was used to reduce the γ-ray self-absorption factor, which otherwise could be significant and would have to be taken into account. The same procedure was used for thick gold samples.

The beta counting was done in 2π and 4π windowless proportional flow counters. The plateau was determined at regular intervals. In addition, the count rate of a depleted uranium source was checked each time the counter was used.

The relative counting efficiency ϵ_c/ϵ_b (eq. (2)) is of concern when beta particles from thick samples are counted. The W^{185} isotope is distributed nonuniformly throughout both the cadmium-covered and the bare samples because of neutron self-shielding. The counting efficiency depends on β-ray self-absorption and scattering, which, in turn, depends on the distribution of W^{185} in the sample.

To determine ϵ_c/ϵ_b for thick foils, the foils were dissolved after irradiation in ZPR-1 and thus transformed into a homogeneous form suitable for beta counting. The dissolved samples were converted into stock solutions of sodium tungstate of 20 grams each. After the W^{187} activity had decayed, the solutions were counted in 1-gram amounts in an O-ring-sealed holder which was placed in a $2\pi\beta$ windowless proportional counter.

A second method that was used to determine the bare and cadmium-covered beta-counting efficiencies consisted of preparing thin samples from activated thick samples. Determination of the disintegration rate was done by using very thin samples, thereby reducing self-absorption and self-scattering. The samples were mounted on thin backing consisting of gold-coated plastic film (such as described in ref. 17, p. 343) and were counted in 4π geometry. The geometry, the beta self-absorption and scattering factors, and the mount absorption and scattering factors were taken to be one.

RESULTS

Dilute Resonance Integrals of Tungsten 186 and Tungsten 184

The results of the cadmium-ratio determinations for the thin films are shown in table II. The bare and cadmium-covered saturated count rates are adjusted to the reactor power indicated by the gold monitor foils mentioned previously. The errors shown in the table are based on the counting statistics for both the foil and the monitor foil. Activity due to the impurities in the aluminum backing was small compared with W^{187}, but its subtraction was significant in determining the W^{185} activity. For sample 2, only the cadmium ratio for W^{186} was determined because of contamination that was large enough to interfere with the W^{184} determination. All count rates except those for sample 8 were obtained from beta counting. The high gold count rate relative to tungsten for sample 8 made the W^{187} beta count rate highly uncertain. The count rates listed for this sample were obtained by counting the 0.68-MeV (1.09×10^{-19} J) γ-ray from W^{187}, and the 0.41 MeV (6.56×10^{-20} J) γ-ray from Au^{198}. Effective resonance integral values listed in the last column of table II are based on a dilute resonance integral for gold of 1570±40 barns ($(1.57\pm0.04)\ 10^{-25}$ m^2), and the values listed in table III. The resonance integral of W^{186} was increased by 2 percent because of the cadmium resonance shielding

of the 18.8-electron-volt (3.01×10^{-18} J) resonance.

The average I_{eff} values for the samples with sample size $(S/M)^{1/2}$ values greater than 100 are 443±17 barns ((4.43±0.17) 10^{-26} m^2) for W^{186} and 15.0±1.8 barns ((1.5±0.18) 10^{-27} m^2) for W^{184}.

Gold 197 Capture Ratio in Thick Metal Foils and Vacuum-Deposited Films

Table IV shows the relative γ-ray specific count-rate values for a series of cadmium-covered gold foils and films of varying thickness. All four samples are 2.54 centimeters in diameter. Samples 9 and 10 consist of gold metal vacuum deposited on 0.0025-centimeter-thick aluminum. The effective resonance integral I_{eff} is obtained by normalizing to the infinitely dilute resonance integral value of 1570±40 barns ((1.57±0.04) 10^{-25} m^2).

Tungsten 186 Capture Rates in Thick Metal Foils and Electroplated Films

Relative γ-ray specific count-rate values for a series of cadmium-covered foils and films of varying thickness are shown in table V. Samples A, B, and C consist of natural tungsten electroplated on 5.62-centimeter-diameter by 0.08-centimeter-thick aluminum. Samples E, G, and I are natural tungsten foils 0.0025, 0.0075, and 0.012 centimeter thick, respectively, with the same diameter as the films. Samples D, F, H, J, and K are rectangular samples. Samples J and K consist of 0.012-centimeter-thick samples stacked together to give the $(S/M)^{1/2}$ values presented. The specific count-rate values given in column 4 were adjusted to the same reactor power by gold monitors. The effective resonance integral I_{eff} was obtained by averaging the specific count rates for samples A, B, and C and normalizing them to the dilute sample average of 443 barns (4.43×10^{-26} m^2) (table II).

Thick-Sample Tungsten 184 Resonance Integral

Results of the 0.0127-centimeter-thick cadmium ratio determinations are shown in table VI. Samples M and N were calibrated, using W^{187} activity, by exposing them at identical times to the same flux from the ZPR-1 core. The calibration was accomplished by mounting the cadmium-shielded foils on a rotating wheel and exposing them to the flux, gamma counting them, and then repeating the procedure without cadmium. The amount of W^{185} activity induced in the calibration runs was insignificant. The foil calibration

results showed that the response of the foils to both epicadmium and bare neutrons was the same, within 2 percent. This variation was included as an additional uncertainty. A gold foil, 0.00254-centimeter-thick and 5.08 centimeters in diameter, was chosen to match the effective thermal absorption of the 0.0127-centimeter-thick natural tungsten samples. If Σ_{th} = 1.13 per centimeter for tungsten and Σ_{th} = 5.82 per centimeter for gold obtained from thermal cross section values reported in reference 9 are used, a thickness of 0.00247 centimeter is required to match the thermal absorption in the tungsten exactly. The values are close enough to ensure that the thermal flux was the same for both gold and tungsten to within a power factor so that the effective thermal cross sections in equation (4) may be replaced by the thermal cross sections for infinitely thin samples.

A value of 590±10 barns ((5.90±0.10) 10^{-26} m^2) for the resonance integral of gold was computed from the resonance parameters. Sample L was used for both bare and cadmium-shielded activations. Sample M was irradiated bare in the center of ZPR-1, while sample N was irradiated in cadmium. These were natural tungsten foils 5.08 centimeters in diameter and 0.013 centimeter thick. Surface to mass ratio values for samples M and N determined from weight and area differed by no more than 1 percent, and an average value was used. The count rate values for W^{185} were obtained by solution counting.

The uncertainties in the relative power adjustments are reflected in the errors given in table VI for the bare activities. Beta count rates of the solutions were extrapolated to the end of irradiation and averaged to give the value in column 4. The end-of-irradiation beta count rates for W^{185} in the undissolved samples are given in table VII. These rates give a ratio R' without the efficiency factor of 2.79, a difference of about 5.0 percent from the solution cadmium ratio, which apparently results from the effect of ϵ_c/ϵ_b (eq. (2)). Samples BP and CP, also 0.0127 centimeter thick, were exposed bare and cadmium-shielded in the Plum Brook reactor. Disintegration rates of W^{185} per unit mass were determined by the method described in the section Counting Method. The efficiency ratios given in the last column of table VII indicate again that the cadmium ratio obtained by taking whole-sample beta counts is too low. The results obtained for samples BP and CP have low precision, which is caused primarily by difficulties in determining the mass vacuum deposited on the thin film backing.

Comparison With Computed Values

The resonance integral values for gold, W^{184}, and W^{186} are shown as functions of sample size $(S/M)^{1/2}$ in figure 4. The curves are values computed by the Nordheim integral code mentioned previously, to which 1/v and unresolved contributions were added.

Gold 197. - The parameters for the gold resonances up to 940 electron volts (1.51×10^{-16} J) are reported in reference 18. The uncertainties in both Γ_n and Γ_γ for the 4.9-electron-volt (7.8×10^{-19} J) resonance are reported to be 2.5 percent. This resonance accounts for 93 percent of the dilute resonance integral. The uncertainty in the parameters for the rest of the resolved resonances is in most cases less than 20 percent. The gold data resulting from the relative activation method have errors of approximately 3 percent for each of the samples measured. These data, normalized to the dilute calculated resonance integral, are shown in figure 4(a). The agreement is good throughout the range of thicknesses.

Tungsten 184. - The W^{184} calculation and data are shown in figure 4(b). The lowest curve in the figure is based on a value for the radiation width for all resonances of 0.047 electron volt (7.52×10^{-21} J), which is suggested in reference 19 and obtained by averaging previously reported radiation widths for W^{182} and W^{186}. A value of 0.057 electron volt (9.13×10^{-21} J) for Γ_γ for each resonance yields much better agreement with the measured values. The upper curve, which uses $\Gamma_\gamma = 0.066$ electron volt (1.06×10^{-20} J), also agrees within the uncertainty. The neutron spectroscopic values for Γ_n are insensitive to a chosen value of Γ_γ. This experiment shows that if a value of 0.062 electron volt (9.93×10^{-21} J) is chosen for Γ_γ for all the resonances of W^{184}, agreement is obtained between calculated and measured resonance integrals for this isotope. There is uncertainty in the higher angular momentum contributions, but because of the high energies at which these become effective, their total contribution to the resonance integral is small.

Tungsten 186. - In figure 4(c), the thin sample points obtained by cadmium ratio measurements give an average of 443±17 barns ($(4.43\pm0.17)10^{-26}$ m^2) for the resonance integral. A value for the radiation width of 0.041 electron volt (6.56×10^{-21} J) provides the best agreement with the experimental points. This value should be good for Γ_γ because Γ_n has been measured by spectroscopy with good precision (ref. 20). Also, the 18.8-electron-volt (3.01×10^{-18} J) resonance contributes 92 percent of the total resonance integral.

The measured dilute resonance integral for W^{186} agrees within the uncertainty with the value obtained by various authors when adjustment is made to the values of thermal cross section and dilute resonance integral for gold used herein. Table VIII lists the experimental values obtained for W^{186} together with other pertinent parameters used by various authors. If values of σ_{th} equal to 37.8 barns (3.78×10^{-27} m^2) and I_∞^{Au} equal to 1570 barns (1.57×10^{-25} m^2) are used, Jacks' value (ref. 21) becomes 444 barns (4.44×10^{-26} m^2) and that of Harris, Muelhause, and Thomas (ref. 22) becomes 392 barns (3.92×10^{-26} m^2). The value obtained by Baumann (ref. 23), 394 barns (3.94×10^{-26} m^2), becomes 436 barns (4.36×10^{-26} m^2). This value agrees with the present experiment. Beller and Latham (ref. 24) also give a value in agreement with the present experiment.

The value of 490±50 barns ($(4.90\pm0.5)\,10^{-26}$ m^2) resulting from the boron filter experiment, which when adjusted becomes 542±50 barns ($(5.42\pm0.5)\,10^{-26}$ m^2), is higher than that resulting from the cadmium filter experiments. This discrepancy is not accounted for by cadmium resonance overlap with the 18.8-electron-volt (3.01×10^{-18} J) resonance of W^{186} based on the calculation shown herein.

The thicker samples indicate that the resonance integral decreases with decreasing surface to mass ratio at a greater rate than that shown by the calculations. Tungsten 186 is an unusual case in that it has a low energy resonance with a scattering width much larger than the radiation width. The calculations assume a flat flux over the sample, which is a poor assumption for this isotope. Indications are that this assumption together with shielding by the 21.2-electron-volt (3.38×10^{-18} J) resonance of W^{182} can account for the deviation of the calculated values from the measured values. In reference 6, the contribution of the 18.8-electron-volt (3.01×10^{-18} J) resonance was computed first by using a fine spatial mesh in the lump and then by assuming a hyperbolic cosine variation for the flux. In each case, the resulting integral was lower by about 13 percent for an S/M of 1.00 for natural tungsten and by 6 percent for an S/M of 6.25 for natural tungsten.

CONCLUSIONS

Resonance capture integrals referred to gold as a standard were measured for tungsten 184 and tungsten 186 by the activation technique. Results for the dilute resonance integral are 443±17 barns ($(4.43\pm0.17)\,10^{-26}$ m^2) for tungsten 186 and 15.0±2 barns ($(1.50\pm2.0)\,10^{-27}$ m^2) for tungsten 184. Calculations show that cadmium shielding of the 18.8-electron-volt (3.01×10^{-18} J) resonance of tungsten 186 results in a 2- to 3-percent correction to the measured dilute resonance integral. Measured resonance integrals for thick samples, when compared with calculated resonance integrals, show a significant difference for tungsten 186. This variation is attributed to approximations made in the calculation. A half-life measurement of tungsten 185 yielded a value of 76.4±0.7 days.

Lewis Research Center,
National Aeronautics and Space Administration,
Cleveland, Ohio, April 18, 1967,
129-02-04-04-22.

APPENDIX A

SYMBOLS

B	saturated count rate for bare sample, counts/min
C	saturated count rate for cadmium shielded sample, counts/min
E	neutron energy, eV (J)
E_{Cd}	lower energy limit standardized to 0.5 eV (8.01×10^{-20} J) or cadmium cutoff energy
I_{eff}	effective resonance integral, b (m^2)
$(I_{eff})_{calc}$	total calculated resonance integral for 1/E flux down to 0.5 eV (8.01×10^{-20} J), b (m^2)
$(I_{eff})_g$	group contribution to effective resonance integral, b (m^2)
I_∞	infinitely dilute resonance integral, b (m^2)
R	cadmium ratio
R'	cadmium ratio without efficiency factor
r	spatial coordinate
S/M	surface to mass ratio of sample, cm^2/g
$T(E)$	transmission probability for neutron flux of energy E
u	lethargy
v	neutron velocity
Γ_n	neutron scattering width of resonance, eV (J)
Γ_γ	neutron capture (or radiation) width of resonance, eV (J)
ϵ_b	counting efficiency of bare sample
ϵ_c	counting efficiency of cadmium-shielded sample
μ	calculated correction factor to resonance integral
$\Sigma_a(E)$	macroscopic capture cross section, b (m^2)
$\sigma_a(E)$	Doppler broadened neutron capture cross section, b (m^2)
σ_{th}	thermal capture cross section at 0.025 eV, b (m^2)
$(\sigma_{th})_{eff}$	effective thermal capture cross section, b (m^2)
τ	thickness of shield or sample, cm
φ_b	flux at center of ZPR-1, no cadmium
φ_c	flux within cadmium shield at center of ZPR-1
$(\varphi_b)_g$	flux for energy group g at center of ZPR-1, no cadmium

$(\varphi_c)_g$ flux for energy group g within cadmium shield, at center of ZPR-1

$\varphi(u)$ flux at center of ZPR-1 as function of lethargy

Superscripts:

Au gold

Cd^{113} cadmium 113

g energy group g

s standard sample

W tungsten

W^{186} tungsten 186

x isotope under investigation

Subscripts:

eff effective

m I_{eff}/μ

APPENDIX B

EFFECT OF NEUTRON FLUX IN RESONANCE INTEGRAL MEASUREMENT

In terms of flux and cross sections R^X can be written as

$$R^X = \frac{\int_r \int_0^\infty \sigma_a^X(E)\varphi_b(E,r)dE\ dr}{\int_r \int_{0.41}^\infty \sigma_a^X(E)\varphi_c(E,r)dE\ dr} \tag{6}$$

where σ_a is the Doppler broadened neutron capture cross section for the material, and φ_b and φ_c are the flux without and with the cadmium shield in the center of ZPR-1. Since gold is used as the standard, the flux is normalized to a value of 1 at the major resonance of gold, 4.9 electron volts (7.85×10^{-19} J). For dilute samples, this resonance accounts for 93 percent of the resonance integral of gold. The arbitrary lower limit of 0.41 electron volt (6.56×10^{-20} J) is such that the flux is essentially zero inside the cadmium shield, as shown in figure 1, where 0.41 electron volt (6.56×10^{-20} J) corresponds to a lethargy of 17. In this experiment, both the bare and cadmium-shielded samples have the same dimensions and occupy the same position during the irradiations.

The numerator in equation (6) may be separated into two parts. The energy variation of φ_b is known for lethargies less than 17, as shown in figure 1. Therefore, the separation is made at this point. Then

$$R^X = \frac{\int_r \int_0^{0.41} \sigma_a^X(E)\varphi_b(E,r)dE\ dr + \int_r \int_{0.41}^\infty \sigma_a^X(E)\varphi_b(E)\ dE}{\int_r \int_{0.41}^\infty \sigma_a^X(E)\varphi_c(E,r)dE}$$

$$= \frac{\int_r \int_0^{0.41} \sigma_a^X(E)\varphi_b(E,r)dE\ dr}{\int_r \int_{0.41}^\infty \sigma_a^X(E)\varphi_c(E,r)dE} + \frac{\int_r \int_{0.41}^\infty \sigma_a^X(E)\varphi_b(E,r)dE}{\int_r \int_{0.41}^\infty \sigma_a^X(E)\varphi_c(E,r)dE} \tag{7}$$

For the samples used in this experiment, the second term on the right side is very close to 1. To see this, let

$$\int_r \int_{0.41}^{\infty} \sigma_a^x(E)\varphi_c(E,r)dE = \sum_g (I_{eff}^x)_g (\varphi_c)_g \tag{8}$$

and

$$\int_r \int_{0.41}^{\infty} \sigma_a^x(E)\varphi_b(E,r)dE = \sum_g (I_{eff}^x)_g (\varphi_b)_g \tag{9}$$

where the sums range in energy from 0.41 electron volt (6.56×10^{-20} J) to infinity and where $(\varphi_b)_g$ and $(\varphi_c)_g$ are the calculated fluxes for energy group g in the center of ZPR-I, without and with the cadmium shield. The calculated group contribution to the resonance integral is $(I_{eff})_g$, when an incident 1/E flux is assumed and when self-shielding is taken into account, if such exists. In the actual calculation, the sums may be terminated at some high-energy (low lethargy) value.

Figure 1 indicates that the major difference between φ_b and φ_c lies at lethargies above 15 and that higher-energy resonances in cadmium have little effect on the flux group values (an overlap of resonances in Cd^{113} and W^{186} is treated in the section on Method and Analysis). Tables IX and X illustrate the procedure. The complete slowing-down interval was divided into groups, and the calculated group values for the absorption integral were multiplied by the corresponding group values for the flux. Low-energy cross sections obtained from reference 9 were used to calculate I_{eff} for the regions from 0.41 and 0.50 electron volt (6.56×10^{-20} and 8.01×10^{-20} J) to the first resonance. The sources for resonance parameters used for the resolved region are given at the end of this appendix. Booth, Ball, and MacGregor (ref. 25) present measured values of 0.27 and 0.35 barn (2.7×10^{-29} and 3.5×10^{-29} m^2), respectively, for the (n, γ) cross sections of W^{186} and W^{184} at 24 kiloelectron volts (3.84×10^{-15} J). This result is higher than the calculated s-wave contribution. Therefore, p-wave contributions were calculated and added in as indicated.

The $I_{eff}\varphi(u)$ values cover the energy range from 0.41 to 10.0×10^{6} electron volts (6.56×10^{-20} to 1.60×10^{-13} J). Results for smaller values of S/M are presented in condensed forms in tables VII and VIII.

For W^{186}, $\sum_g (I_{eff})_g (\varphi_b)_g \Big/ \sum_g (I_{eff})_g (\varphi_c)_g$ is 1.004. The $I_{eff}\varphi_b(u)$ values for W^{184} and the $I_{eff}\varphi_b(u)$ and $I_{eff}\varphi_c(u)$ values for gold^{197} are not shown in the tables, but the ratios are 1.006 and 1.005, respectively. These values are very close to 1; and they may be taken to be 1.

Then

$$R^x - 1 = \frac{\int_r \int_0^{0.41} \sigma_a^x(E)\varphi_b(E, r)dr}{\left(I_{eff}^x\right)_m} \tag{10}$$

where

$$\int_r \int_{0.41}^{\infty} \sigma_a^x(E)\varphi_c(E, r)dE = \left(I_{eff}^x\right)_m \tag{11}$$

There is a similar expression for the gold standard. Then,

$$\left(I_{eff}^x\right)_m = \frac{\int_r \int_0^{0.41} \sigma_a^x(E)\varphi_b(E, r)dr}{\int_r \int_0^{0.41} \sigma_a^{Au}(E)\varphi_b(E, r)dr} \frac{R^{Au} - 1}{R^x - 1} \left(I_{eff}^{Au}\right)_m \tag{12}$$

Thermal flux depression is negligible for very thin samples. For thicker samples, the gold thickness may be chosen so that the thermal flux depression is the same for the gold standard as for the natural tungsten sample. Then, if the absorption cross sections have the same energy dependence from 0 to 0.41 electron volt (0 to 6.56×10^{-20} J),

$$\frac{\int_r \int_0^{0.41} \sigma_a^x(E)\varphi_b(E, r)dr}{\int_r \int_0^{0.41} \sigma_a^{Au}(E)\varphi_b(E, r)dr} = \frac{\sigma_{th}^x}{\sigma_{th}^{Au}} \tag{13}$$

The quantities $(I_{eff})_m$ must be corrected for a variation of the flux with lethargy and a cutoff energy that is different from 0.5 electron volt (8.01×10^{-20} J). Therefore,

$$I_{eff} = \mu\left(I_{eff}\right)_m \tag{14}$$

where

$$\mu = \frac{(I_{eff})_{calc}}{\Sigma_g (I_{eff})_g (\rho_c)_g} \tag{15}$$

where $(I_{eff})_{calc}$ is the total calculated resonance integral for a $1/E$ flux down to 0.5 electron volt (8.01×10^{-20} J) and g carries the neutron spectrum down to 0.41 electron volt (6.56×10^{-20} J).

For fairly thin gold samples, μ is very nearly 1 and is taken to be 1. The factor differs from 1 by a negligible amount because of the strong resonance at 4.9 electron volts (7.85×10^{-19} J) and the fact that the reduction in the 1/v component offsets the increased importance of the higher-energy contributions (ref. 3). The correction factor μ is 0.955 for W^{186} and 0.886 for W^{184} for the dilute cases. Most of the correction is caused by the difference in energy location of the major contributing resonances. These energies are quite accurate. Varying the resonance parameters somewhat should have little effect on the correction factor.

The resonance parameters used in obtaining the calculated correction factors are tabulated in reference 3. Most of the resonance parameters used for computing I_{eff} in table IX for W^{186} were obtained from reference 20. The parameters for the main resonance (18.8 eV (3.01×10^{-18} J)) of W^{186} were taken to be $\Gamma_n = 0.319$ electron volt (5.11×10^{-20} J) (ref. 26), and $\Gamma_\gamma = 0.0442$ electron volt (7.08×10^{-21} J), where the value for Γ_γ was calculated by using the Γ_n given and the thermal absorption cross section value of 37.8±1.2 barns ((3.78±0.12) 10^{-27} m^2) measured by Friesenhahn, et al. (ref. 9). The next higher energy resonance is at 171.5 electron volts (2.75×10^{-12} J), and its contribution to the thermal cross section is small. Parameters for W^{184} (table X) were taken mostly from reference 19. A value of 0.057 electron volt (9.13×10^{-21} J) was used for the radiation width for all resonances and a thermal cross section of 1.7±0.1 barns ((1.7±0.1) 10^{-28} m^2) was obtained (ref. 9).

REFERENCES

1. Bogart, D.; and Lantz, E.: Nuclear Physics of Solid-Core Gas-Cooled Rocket Propulsion Reactors. Proceedings of the NASA-University Conference on the Science and Technology of Space Exploration. NASA SP-11, Vol. 2, 1962, pp. 77-85.

2. Scoville, J. J.; Knight, D. W.; and Fast, E.: Resonance Absorption Integrals of Dysprosium and Tungsten. Am. Nucl. Soc. Trans., vol. 5, no. 2, Nov. 1962, pp. 377-378.

3. Shook, Donald F.; and Bogart, Donald: Effective Resonance Integrals of Separated Tungsten Isotopes. NASA TN D-3957, 1967.

4. Nordheim, L. W.: A New Calculation of Resonance Integrals. Nucl. Sci. Eng., vol. 12, no. 4, Apr. 1962, pp. 457-463.

5. Kuncir, G. F.: A Program for the Calculation of Resonance Integrals. Rep. No. GA-2525, General Atomic Div., General Dynamics Corp., Aug. 28, 1961.

6. Cohen, Sanford C.: An Improved Treatment of Scattering Resonances in Slab Geometry. Nucl. Sci. Eng., vol. 27, no. 1, Jan. 1967, pp. 133-135.

7. Westfall, Robert M.: Resonance Overlap in Natural Tungsten. Am. Nucl. Soc. Trans., vol. 9, no. 2, Nov. 1966, pp. 504-505.

8. Macklin, R. L.; and Pomerance, H. S.: Resonance Capture Integrals. Physics of Reactor Design. Vol. 5 of the Proceedings of the International Conference on the Peaceful Uses of Atomic Energy, Geneva, Aug. 8 - Aug. 20, 1955, United Nations, 1956, pp. 96-101.

9. Friesenhahn, S. J.; Haddad, E.; Fröhner, F. H.; and Lopez, W. M.: The Neutron Capture Cross Section of the Tungsten Isotopes from 0.01 to 10 Electron Volts. Nucl. Sci. Eng., vol. 26, no. 4, Dec. 1966, pp. 487-499.

10. Fieno, Daniel: Transport Study of the Real and Adjoint Flux for NASA Zero Power Reactor (ZPR-1). NASA TN D-3990, 1967.

11. Joanou, G. D.; and Dudek, J. S.: GAM-II. A B_3 Code for the Calculation of Fast-Neutron Spectra and Associated Multigroup Constants. Rep. No. GA-4265, General Atomic Div., General Dynamics Corp., Sept. 16, 1963.

12. Drake, M. K.: Neutron Cross Sections for Cadmium Isotopes. Rep. No. GA-6997 (NASA CR-54933), General Atomic Div., General Dynamics Corp., Mar. 25, 1966.

13. Abramowitz, Milton; and Stegun, Irene A., eds.: Handbook of Mathematical Functions with Formulas, Graphs, and Mathematical Tables. Appl. Math. Series 55, NBS, June 1964.

14. Hallman, T. M.; and Lubarsky, B.; eds.: NASA Reactor Facility Hazards Summary. Vol. I. NASA Memo 12-8-58E, Jan. 1959.

15. Sen Gupta, A. K.; Comp.: A = 185. Ta, W, Re, Os, Ir, Pr, Au, Hg. Nuclear Data, vol. 1, no. 1, Feb. 1966, p. B1-1-85.

16. Neumann, Gerhard M.; and Hirschwald, Wolfgang: Zur Halbwertszeit von Wolfram - 185. Nukleonik, vol. 8, no. 8, Nov. 1966, p. 484.

17. Siegbahn, Kai, ed.: Alpha-Beta- and Gamma-Ray Spectroscopy. Vol. 1, North-Holland Pub. Co., Amsterdam, 1965.

18. Desjardins, J. S.; Rosen, J. L.; Havens, W. W., Jr.; and Rainwater, J.: Slow Neutron Resonance Spectroscopy. II. Ag, Au, Ta. Phys. Rev., vol. 120, no. 6, Dec. 15, 1960, pp. 2214-2226.

19. Khan, F. A.; and Harvey, J. A.: Parameters of Neutron Resonances in ^{184}W. Nucl. Sci. Eng., vol. 25, no. 1, May 1966, pp. 31-36.

20. Block, R. C.; Hockenberry, R. W.; and Russell, J. E.: The Parameters of the Neutron Resonances in ^{182}W, ^{183}W, ^{184}W, and ^{186}W, Oak Ridge Nat. Lab. Physics Div. Ann. Progress Rep. for Dec. 1965, ORNL-3924, May 1966.

21. Jacks, George M.: A Study of Thermal and Resonance Neutron Flux Detectors. Rep. No. DP-608, E. I. DuPont de Nemours & Co., Aug. 1961.

22. Harris, S. P.; Muehlhause, C. O.; and Thomas, G. E.: Low Energy Neutron Resonance Scattering and Absorption. Phys. Rev., vol. 79, no. 1, July 1, 1950, pp. 11-18.

23. Baumann, Norman P.: Resonance Integrals and Self-Shielding Factors for Detector Foils. Rep. No. DP-817, E. I. DuPont de Nemours & Co., Jan. 1963.

24. Beller, L. S.; and Latham, D. W.: The Infinitely Dilute Resonance Integral of Tungsten-186. Am. Nucl. Soc. Trans., vol. 9, no. 1, June 1966, pp. 247-248.

25. Booth, Rex; Ball, William P.; and MacGregor, Malcolm H.: Neutron Activation Cross Sections at 25 KeV. Phys. Rev., vol. 112, no. 1, Oct. 1, 1958, pp. 226-229.

26. Harvey, J. A.: The Measurement of Total Neutron Cross Sections in the Resonance Energy Region and the Determination of Resonance Absorption. Rep. no. ORNL-P-1885 Oak Ridge National Lab., Jan. 1, 1960.

TABLE I. - CALCULATED SHIELDING OF 18.83-ELECTRON-VOLT (3.014×10^{-18} J) RESONANCE OF TUNGSTEN 186

(a) U.S. Customary Units

Resonance of cadmium 113 at 18.5 electron volts			Transmission probability, T	Neutron capture cross section for tungsten 186, $\sigma_{a}^{W^{186}}$, b	Product of transmission probability and neutron capture cross section for tungsten 186, $T\sigma_{a}^{W^{186}}$, b	Resonance of cadmium 113 at 18.8 electron volts		
Neutron energy, E, eV	Neutron capture cross section for cadmium 113, $\sigma_{a}^{Cd^{113}}$, b	Product of macroscopic capture cross section and sample thickness, $\Sigma_a\tau$				Neutron energy, E, eV	Neutron capture cross section for tungsten 186, $\sigma_{a}^{W^{186}}$, b	Product of transmission probability and neutron capture cross section for tungsten 186, $T\sigma_{a}^{W^{186}}$, b
18.2	8.2	0.0041	0.992	1 150	1 140	18.5	3 550	3 520
18.25	13.5	.0067	.987	1 325	1 310	18.55	4 500	4 440
18.3	27.5	.0137	.974	1 575	1 530	18.6	5 700	5 550
18.35	35	.0174	.967	1 900	1 840	18.65	7 400	7 150
18.4	64	.0319	.941	2 300	2 160	18.7	9 500	8 940
18.45	80	.0398	.927	2 850	2 640	18.75	11 500	10 650
18.5	89	.0443	.919	3 550	3 260	18.8	12 800	11 750
18.55	80	.0398	.927	4 500	4 170	18.85	13 000	12 050
18.6	64	.0319	.941	5 700	5 360	18.9	11 800	11 100
18.65	35	.0174	.967	7 400	7 150	18.95	9 900	9 570
18.7	27.5	.0137	.974	9 500	9 250	19.0	7 700	7 500
18.75	13.5	.0067	.987	11 500	11 500	19.05	6 000	5 920
18.8	8.2	.0041	.992	12 800	12 700	19.1	4 700	4 660
Partial integral, b				159	150		276	263
Reduction based on $I_{\infty}^{W^{186}}$ = 476 b, percent				2			3	

(b) S I Units

Resonance of cadmium 113 at 29.64×10^{-19} joule			Transmission probability, T	Neutron capture cross section for tungsten 186, $\sigma_{a}^{W^{186}}$, m^2	Product of transmission probability and neutron capture cross section for tungsten 186, $T\sigma_{a}^{W^{186}}$, m^2	Resonance of cadmium 113 at 30.12×10^{-19} joule		
Neutron energy, E, eV	Neutron capture cross section for cadmium 113, $\sigma_{a}^{Cd^{113}}$, m^2	Product of macroscopic capture cross section and sample thickness, $\Sigma_a\tau$				Neutron energy, E, J	Neutron capture cross section for tungsten 186, $\sigma_{a}^{W^{186}}$, m^2	Product transmission probability and neutron capture cross section for tungsten 186, $T\sigma_{a}^{W^{186}}$, m^2
29.16×10^{-19}	8.2×10^{-28}	0.0041	0.992	$1\,150\times10^{-28}$	$1\,140\times10^{-28}$	29.64×10^{-19}	$3\,550\times10^{-28}$	$3\,520\times10^{-28}$
29.24	13.5	.0067	.987	1 325	1 310	29.72	4 500	4 440
29.32	27.5	.0137	.974	1 575	1 530	29.80	5 700	5 550
29.40	35	.0174	.967	1 900	1 840	29.88	7 400	7 150
29.48	64	.0319	.941	2 300	2 160	29.96	9 500	8 940
29.56	80	.0398	.927	2 850	2 640	30.04	11 500	10 650
29.64	89	.0443	.919	3 550	3 260	30.12	12 800	11 750
29.72	80	.0398	.927	4 500	4 170	30.20	13 000	12 050
29.80	64	.0319	.941	5 700	5 360	30.28	11 800	11 100
29.88	35	.0174	.967	7 400	7 150	30.36	9 900	9 570
29.96	27.5	.0137	.974	9 500	9 250	30.44	7 700	7 500
30.04	13.5	.0067	.987	11 500	11 500	30.52	6 000	5 920
30.12	8.2	.0041	.992	12 800	12 700	30.60	4 700	4 660
Partial integral, m^2				1.59×10^{-26}	1.50×10^{-26}		2.76×10^{-26}	2.63×10^{-26}
Reduction based on $I_{\infty}^{W^{186}}$ = 4.76×10^{-26} m^2, percent				2			3	

TABLE II. - TUNGSTEN 186 AND TUNGSTEN 184 DILUTE RESONANCE INTEGRALS OBTAINED FROM VACUUM-DEPOSITED SAMPLES OF TUNGSTEN AND SODIUM TUNGSTATE

Foil	Material	Weight of deposit, mg	Sample size, $(S/M)^{1/2}$, $(cm^2/g)^{1/2}$	Isotope	Cadmium ratio	Effective resonance integral, I_{eff}, eq. (4)	
						b	m^2
1	Gold	1.16	140	Gold 198	1.95±0.05	---	---
2	Sodium tungstate (Na_2WO_4)	6.48	147	Tungsten 186	2.22±0.09	456±47	$(456±47)\times10^{-28}$
3	Gold	.50	179	Gold 198	1.92±0.05	---	---
4	Sodium tungstate (Na_2WO_4)	4.35	150	Tungsten 186	2.20±0.04	450±34	$(450±34)\times10^{-28}$
			144	Tungsten 184	2.54±0.16	14.4±2.0	$(14.4±2.0)\times10^{-28}$
5	Sodium tungstate (Na_2WO_4)	13.9	84	Tungsten 186	2.25±0.07	432±38	$(432±38)\times10^{-28}$
			81	Tungsten 184	2.46±0.05	15.2±1.5	$(15.2±1.5)\times10^{-28}$
6	Tungsten	.07	914	Tungsten 186	2.23±0.33	438±33	$(438±33)\times10^{-28}$
7	Gold plus sodium tungstate	.30	230	Gold 198	1.91±0.03	---	---
		2.89	184	Tungsten 186	2.20±0.04	426±27	$(426±27)\times10^{-28}$
			177	Tungsten 184	2.42±0.11	15.5±1.9	$(15.5±1.9)\times10^{-28}$
8	Gold plus sodium tungstate	.69	152	Gold 198	1.93±0.04	---	---
		1.45	257	Tungsten 186	2.25±0.24	443±94	$(443±94)\times10^{-28}$

TABLE III. - PARAMETERS USED IN DETERMINING EFFECTIVE RESONANCE INTEGRAL FOR TUNGSTEN 186 AND TUNGSTEN 184

Parameter	Sample						Source
	[a]Tungsten 186		[b]Tungsten 184		Gold 197		
	b	m^2	b	m^2	b	m^2	
Thermal capture cross section at 0.025 eV, σ_{th}	37.8±1.2	$(37.8±1.2)\times10^{-28}$	1.7±0.1	$(1.7±0.1)\times10^{-28}$	98.7±1.8	$(98.7±1.8)\times10^{-28}$	Ref. 9

[a]Flux correction factor to resonance integral μ, 0.955.
[b]Flux correction factor to resonance integral μ, 0.886.

TABLE IV. - RELATIVE GOLD 198 SPECIFIC COUNT RATES

Sample	Mass, mg	Sample size, $(S/M)^{1/2}$, $(cm^2/g)^{1/2}$	Specific count rate, counts/(min)(mg)	Effective resonance integral, I_{eff}	
				b	m^2
9	0.118	293.1	95.0±2.5	1570±40	$(1570\pm40)\times10^{-28}$
10	14.899	25.9	76.6±2.3	1265±60	$(1265\pm60)\times10^{-28}$
11	1321.0	2.83	16.9±0.5	279±13	$(279\pm13)\times10^{-28}$
12	7525.9	1.16	8.34±0.2	138±6	$(138\pm6)\times10^{-28}$

TABLE V. - RELATIVE TUNGSTEN 186 SPECIFIC COUNT RATES FOR NATURAL TUNGSTEN FOILS

Sample	Mass, mg	Foil size, cm	Specific count rate, counts/(min)(mg)	Effective resonance integral, I_{eff}	
				b	m^2
A	0.54±0.01	5.36	38.9±2.7	488±35	$(438\pm35)\times10^{-28}$
B	3.70±0.03	5.36	34.6±0.6	434±10	$(434\pm10)\times10^{-28}$
C	4.20±0.09	5.36	36.2±0.9	456±13	$(456\pm13)\times10^{-28}$
D	596.5	5.08 by 3.81	25.2±0.5	316±8	$(316\pm8)\times10^{-28}$
E	1 161.5	5.36	21.5±0.2	270±5	$(270\pm5)\times10^{-28}$
F	3 611.0	5.08 by 3.81	13.3±0.3	167±5	$(167\pm5)\times10^{-28}$
G	6 271.4	5.36	11.6±0.1	146±3	$(146\pm3)\times10^{-28}$
H	8 880	5.08 by 3.81	9.70±0.27	122±4	$(122\pm4)\times10^{-28}$
I	28 606	5.36	6.93±0.07	87±2	$(87\pm2)\times10^{-28}$
J	29 870	5.08 by 3.81	6.13±0.20	77±3	$(77\pm3)\times10^{-28}$
K	104 800	5.08 by 3.81	3.42±0.09	43±1	$(43\pm1)\times10^{-28}$

TABLE VI. - RESONANCE INTEGRALS FOR 0.0127-CENTIMETER-THICK NATURAL TUNGSTEN SAMPLES

Foil	Isotope	Sample size, $(S/M)^{1/2}$, $(cm^2/g)^{1/2}$	Count rate at end of irradiation, counts/min	Cadmium ratio	Effective resonance integral, I_{eff}, eq. (4)	
					b	m^2
L	Gold 197	6.70	[a] $(2.58\pm0.02)\times10^4$	3.22 ± 0.11		
L	Gold 197	6.70	[b] $(8.01\pm0.04)\times10^5$	---	---	---
M	Tungsten 186	5.55	[a] $(5.89\pm0.12)\times10^7$	---	---	---
N	Tungsten 186	5.55	[b] $(1.43\pm0.03)\times10^7$	4.12 ± 0.12	154 ± 12	$(154\pm12)\times10^{-28}$
M	Tungsten 184	5.32	[a] 1630 ± 40	---	---	---
N	Tungsten 184	5.32	[b] 558 ± 12	2.92 ± 0.10	10.3 ± 1.2	$(10.3\pm1.2)\times10^{-28}$

[a] Bare.
[b] Cadmium covered.

TABLE VII. - TUNGSTEN 185 β-RAY COUNTING EFFICIENCIES FOR BARE AND CADMIUM-COVERED 0.0127-CENTIMETER-THICK SAMPLES

Sample	Specific count rate, counts/(min)(g)	Cadmium ratio without efficiency factor, R'	Count rate for solution, counts/(min)(g)	Specific activity, dis/(min)(g)	Cadmium ratio, R	Efficiency ratio
M	$(4.97\pm0.04)\times10^3$	2.79 ± 0.03	1630 ± 4.0	---	2.92 ± 0.10	1.05 ± 0.04
N	$(1.78\pm0.01)\times10^3$	---	558 ± 12	---	---	---
BP	$(1.94\pm0.02)\times10^6$	---	---	$(5.31\pm0.44)\times10^7$	---	---
CP	$(1.84\pm0.02)\times10^5$	10.5 ± 0.2	---	$(4.62\pm0.38)\times10^6$	11.5 ± 1.4	1.10 ± 0.10

TABLE VIII. - EXPERIMENTAL VALUES[a] OF TUNGSTEN-186 RESONANCE INTEGRAL

Method of measurement	Effective resonance of integral of tungsten 186,		Infinitely dilute resonance integral of gold, I_∞^{Au}		Thermal capture cross section of tungsten 186, $\sigma_{th}^{W\,186}$		Thermal capture cross section of gold, σ_{th}^{Au}		Adjusted thermal cross section of tungsten 186, I_{eff}^{W186}		Reference
	b	m^2	b	m^2	b	m^2	b	m^2	b	m^2	
Cadmium ratio	396 ± 59	$(396\pm59)\times10^{-28}$	1558	1558×10^{-28}	34	34×10^{-28}	98.8	98.8×10^{-28}	444 ± 60	$(444\pm60)\times10^{-28}$	21
Cadmium ratio	320 ± 48	$(320\pm48)\times10^{-28}$	1337	1337×10^{-28}	34.2	34.2×10^{-28}	93	93×10^{-28}	392 ± 50	$(392\pm50)\times10^{-28}$	22
Cadmium ratio	394 ± 40	$(394\pm40)\times10^{-28}$	1535	1535×10^{-28}	35	35×10^{-28}	98.8	98.8×10^{-28}	436 ± 40	$(436\pm40)\times10^{-28}$	23
Boron ratio	490 ± 50	$(490\pm50)\times10^{-28}$	1535	1535×10^{-28}	35	35×10^{-28}	98.8	98.8×10^{-28}	542 ± 50	$(542\pm50)\times10^{-28}$	23
Reactivity	449 ± 40	$(449\pm40)\times10^{-28}$	1561	1561×10^{-28}	35	35×10^{-28}	98.8	98.8×10^{-28}	488 ± 40	$(488\pm40)\times10^{-28}$	24
Cadmium ratio	443 ± 17	$(443\pm17)\times10^{-28}$	1570	1570×10^{-28}	37.8	37.8×10^{-28}	98.7	98.7×10^{-28}	443 ± 17	$(443\pm17)\times10^{-28}$	Present report

[a] All values include 1/v component.

TABLE IX. - FLUX WEIGHTED EFFECTIVE RESONANCE INTEGRAL FOR TUNGSTEN 186

(a) U.S. customary units

Energy range, eV	Calculated flux within cadmium shield, $\varphi_c(u)$	Calculated flux without cadmium shield, $\varphi_b(u)$	Sample size, $(S/M)^{1/2}$, $(cm/g)^{1/2}$						
			322			10.2		3.22	
			Effective resonance integral, I_{eff}, b	Flux weighted resonance integral, $I_{eff}\varphi_c(u)$, b	Flux weighted resonance integral, $I_{eff}\varphi_b(u)$, b	Effective resonance integral, I_{eff}, b	Flux weighted resonance integral, $I_{eff}\varphi_c(u)$, b	Effective resonance integral, I_{eff}, b	Flux weighted resonance integral, $I_{eff}\varphi_c(u)$, b
0.50 to 8.07	-----	-----	6.1	-----	-----	6.1	-----	6.1	----
0.41 to 8.07	0.724	0.944	[a]8.2	5.8	7.7	[a]8.2	5.8	[a]8.1	5.8
1.13 to 3.06	.970	.977	6.4	6.2	6.3	6.4	6.2	6.4	6.2
3.06 to 8.07	1.000	1.000	5.4	5.4	5.4	5.4	5.4	5.4	5.4
8.0 to 82	1.047	1.047	445.1	466.0	466.0	227.1	238.0	93.0	97.3
82 to 185	1.084	1.084	2.6	2.8	2.8	2.4	2.6	1.6	1.7
185 to 253	1.101	1.101	4.7	5.2	5.2	3.4	3.7	2.0	2.2
253 to 527	1.105	1.105	2.1	2.3	2.3	1.6	1.8	1.5	1.7
527 to 902	1.121	1.121	1.5	1.7	1.7	1.4	1.6	.9	1.0
902 to 1465	1.134	1.134	.8	.9	.9	.7	.8	.5	.6
1465 to 2170	1.152	1.152	.3	.3	.3	.3	.3	.2	.2
[b]Unresolved s-wave	1.250	1.250	.8	1.0	1.0	.8	1.0	.8	1.0
[c]Higher energy	5.0	5.0	.2	1.0	1.0	.2	1.0	.2	1.0
Total			476.0	498.7	500.7	255.8	268.2	118.2	124.1
Flux correction factor, μ				0.955			0.953		0.952

[a]Not included in total.

[b]Includes estimated p-wave contribution.

[c]Includes estimated s-wave and p-wave contributions.

TABLE IX. - Concluded. FLUX WEIGHTED EFFECTIVE RESONANCE INTEGRAL FOR TUNGSTEN 186

(b) SI units

Energy range, J	Calculated flux within cadmium shield, $\varphi_c(u)$	Calculated flux without cadmium shield, $\varphi_b(u)$	Sample size, $(S/M)^{1/2}$, $(cm/g)^{1/2}$						
			322			10.2		3.22	
			Effective resonance integral, I_{eff}, m^2	Flux weighted resonance integral, $I_{eff}\varphi_c(u)$, m^2	Flux weighted resonance integral, $I_{eff}\varphi_b(u)$, m^2	Effective resonance integral, I_{eff}, m^2	Flux weighted resonance integral, $I_{eff}\varphi_c(u)$, m^2	Effective resonance integral, I_{eff}, m^2	Flux weighted resonance integral, $I_{eff}\varphi_c(u)$, m^2
0.80×10^{-19} to 1.8×10^{-19}	-----	-----	6.1×10^{-28}	----------	----------	6.1×10^{-28}	----------	6.1×10^{-28}	----------
0.66×10^{-19} to 1.81×10^{-19}	0.724	0.944	[a]8.2	5.8×10^{-28}	7.7×10^{-28}	[a]8.2	5.8×10^{-28}	[a]8.1	5.8×10^{-28}
1.81×10^{-19} to 4.70×10^{-19}	.970	.977	6.4	6.2	6.3	6.4	6.2	6.4	6.2
4.90×10^{-19} to 12.92×10^{-19}	1.000	1.000	5.4	5.4	5.4	5.4	5.4	5.4	5.4
1.29×10^{-18} to 13.13×10^{-18}	1.047	1.047	445.1	466.0	466.0	227.1	238.0	93.0	97.3
13.13×10^{-18} to 29.62×10^{-18}	1.084	1.084	2.6	2.8	2.8	2.4	2.6	1.6	1.7
29.62×10^{-18} to 40.50×10^{-18}	1.101	1.101	4.7	5.2	5.2	3.4	3.7	2.0	2.2
40.50×10^{-18} to 84.40×10^{-18}	1.105	1.105	2.1	2.3	2.3	1.6	1.8	1.5	1.7
84.40×10^{-18} to 144.5×10^{-18}	1.121	1.121	1.5	1.7	1.7	1.4	1.6	.9	1.0
144.5×10^{-18} to 234.7×10^{-18}	1.134	1.134	.8	.9	.9	.7	.8	.5	.6
234.7×10^{-18} to 347.5×10^{-18}	1.152	1.152	.3	.3	.3	.3	.3	.2	.2
[b]Unresolved s-wave	1.250	1.250	.8	1.0	1.0	.8	1.0	.8	1.0
[c]Higher energy	5.0	5.0	.2	1.0	1.0	.2	1.0	.2	1.0
Total			476.0	498.7	500.7	255.8	268.2	118.2	124.1
Flux correction factor, μ				0.955			0.953		0.952

[a]Not included in total.

[b]Includes estimated p-wave contribution.

[c]Includes estimated s-wave and p-wave contributions.

TABLE X. - FLUX WEIGHTED EFFECTIVE RESONANCE INTEGRAL FOR TUNGSTEN 184

(a) U.S. customary units

Energy range, J	Calculated flux within cadmium shield, $\varphi_c(u)$	Sample size, $(S/M)^{1/2}$, $(cm/g)^{1/2}$					
		322		10.2		3.22	
		Effective resonance integral, I_{eff}, b	Flux weighted resonance integral, $I_{eff}\varphi_c(u)$, b	Effective resonance integral, I_{eff}, b	Flux weighted resonance integral, $I_{eff}\varphi_c(u)$, b	Effective resonance integral, I_{eff}, b	Flux weighted resonance integral, $I_{eff}\varphi_c(u)$, b
0.50 to 43.7	----	0.69	-----	0.69	-----	0.69	----
0.41 to 43.7	0.72	[a].76	.64	[a].76	0.64	[a].76	0.64
43.7 to 143	1.07	1.03	1.10	1.00	1.07	.87	.93
143 to 248	1.09	6.50	7.09	5.10	5.56	2.79	3.04
248 to 550	1.12	2.07	2.32	1.88	2.11	1.25	1.40
550 to 884	1.14	.82	.93	.72	.82	.47	.54
884 to 1113	1.14	.44	.50	.40	.46	.28	.32
1113 to 1460	1.15	.41	.47	.38	.44	.28	.32
1460 to 2160	1.15	.36	.41	.34	.39	.26	.30
[b]Unresolved s-wave	1.27	1.20	1.53	1.19	1.52	1.14	1.48
[c]Higher energy	3.45	.11	.38	.11	.38	.11	.38
Total		13.63	15.38	11.81	13.39	8.14	8.35
Flux correction factor, μ			0.886		0.880		0.871

[a]Not included in total.

[b]Includes estimated p-wave contribution.

[c]Includes estimated s-wave and p-wave contributions.

TABLE X. - Concluded. FLUX WEIGHTED EFFECTIVE RESONANCE INTEGRAL FOR TUNGSTEN 184

(b) SI units

Energy range, J	Calculated flux within cadmium shield, $\varphi_c(u)$	Sample size, $(S/M)^{1/2}$, $(cm/g)^{1/2}$					
		322		10.2		3.22	
		Effective resonance integral, I_{eff}, m^2	Flux weighted resonance integral, $I_{eff}\varphi_c(u)$, m^2	Effective resonance integral, I_{eff}, m^2	Flux weighted resonance integral, $I_{eff}\varphi_c(u)$, m^2	Effective resonance integral, I_{eff}, m^2	Flux weighted resonance integral, $I_{eff}\varphi_c(u)$, m^2
0.80×10^{-19} to 70.0×10^{-19}	----	0.69×10^{-28}	----------	0.69×10^{-28}	----------	0.69×10^{-28}	----------
0.66×10^{-19} to 70.0×10^{-19}	0.72	[a].76	0.64×10^{-28}	[a].76	0.64×10^{-28}	[a].76	0.64×10^{-28}
7.00×10^{-18} to 22.9×10^{-18}	1.07	1.03	1.10	1.00	1.07	.87	.93
22.9×10^{-18} to 39.7×10^{-18}	1.09	6.50	7.09	5.10	5.56	2.79	3.04
39.7×10^{-18} to 88.1×10^{-18}	1.12	2.07	2.32	1.88	2.11	1.25	1.40
88.1×10^{-18} to 142×10^{-18}	1.14	.82	.93	.72	.82	.47	.54
142×10^{-18} to 178×10^{-18}	1.14	.44	.50	.40	.46	.28	.32
178×10^{-18} to 234×10^{-18}	1.15	.41	.47	.38	.44	.28	.32
234×10^{-18} to 346×10^{-18}	1.15	.36	.41	.34	.39	.26	.30
[b]Unresolved s-wave	1.27	1.20	1.53	1.19	1.52	1.14	1.48
[c]Higher energy	3.45	.11	.38	.11	.38	.11	.38
Total		13.63	15.38	11.81	13.39	8.14	9.35
Flux correction factor, μ			0.886		0.880		0.871

[a]Not included in total.

[b]Includes estimated p-wave contribution.

[c]Includes estimated s-wave and p-wave contributions.

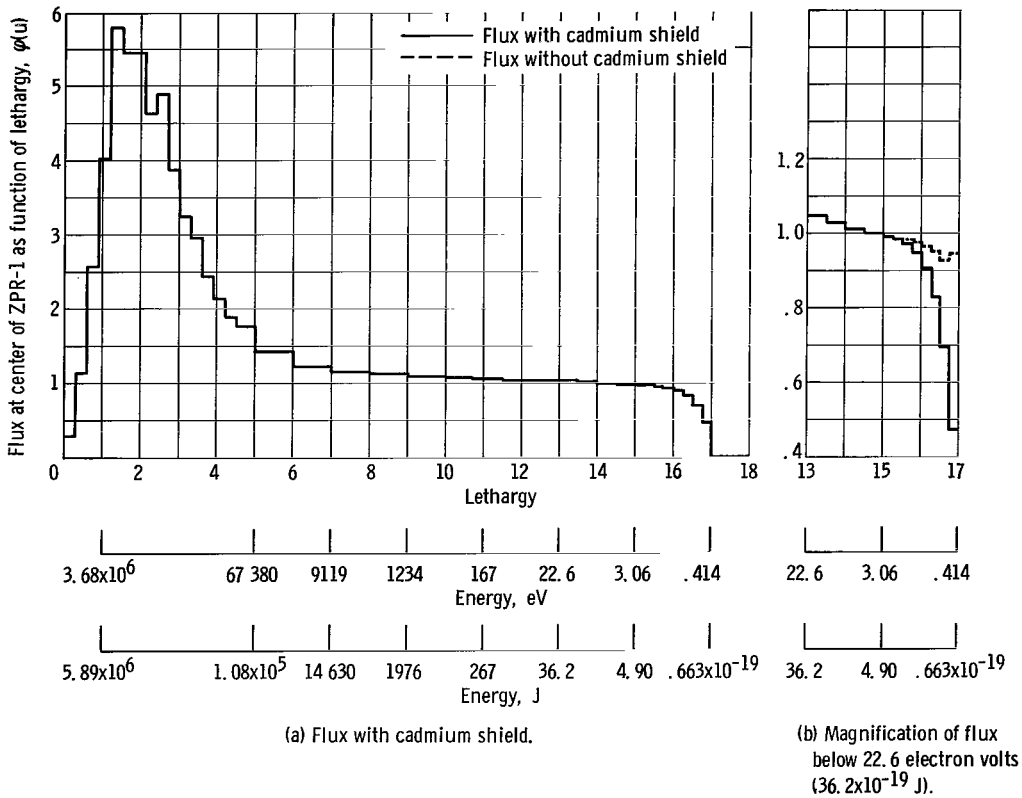

(a) Flux with cadmium shield.

(b) Magnification of flux below 22.6 electron volts (36.2×10^{-19} J).

Figure 1. - Calculated flux at center of ZPR-1 with and without cadmium shield.

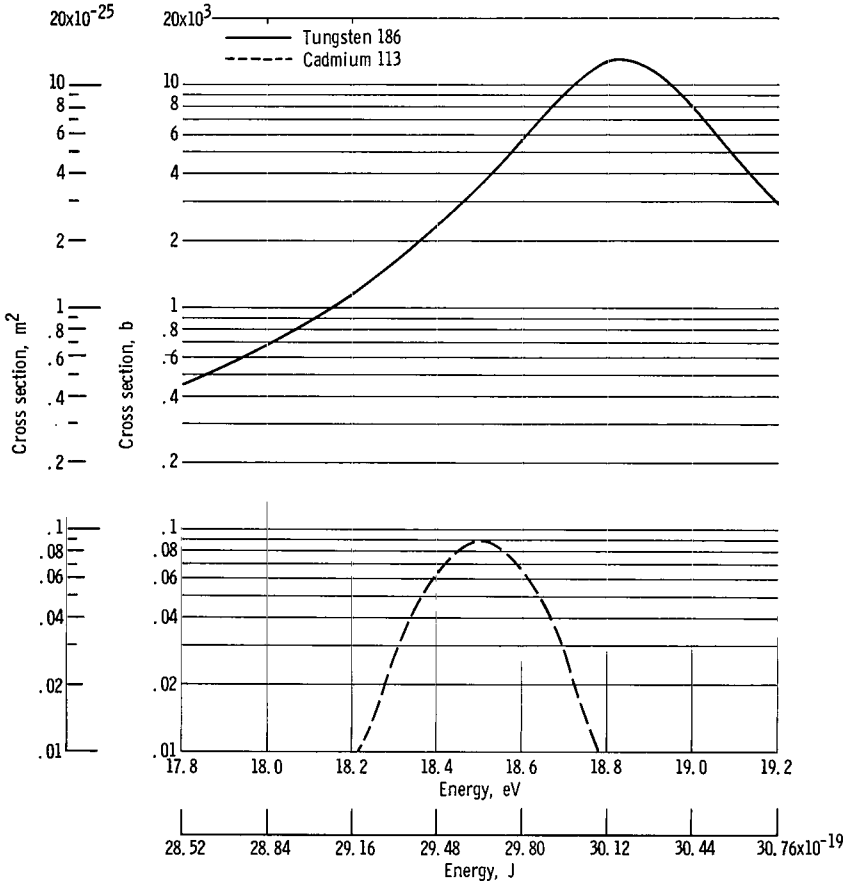

Figure 2. - Overlap of tungsten 186 and cadmium 113 resonances and microscopic Doppler broadened neutron capture cross sections; temperature, 300° K.

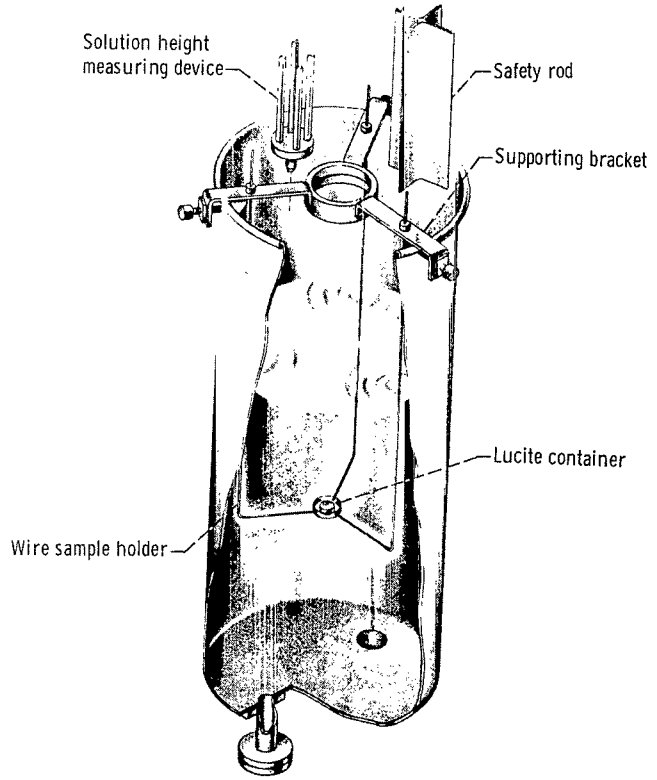

Figure 3. - ZPR-1 reactor tank with foil holder in place for irradiation experiment.

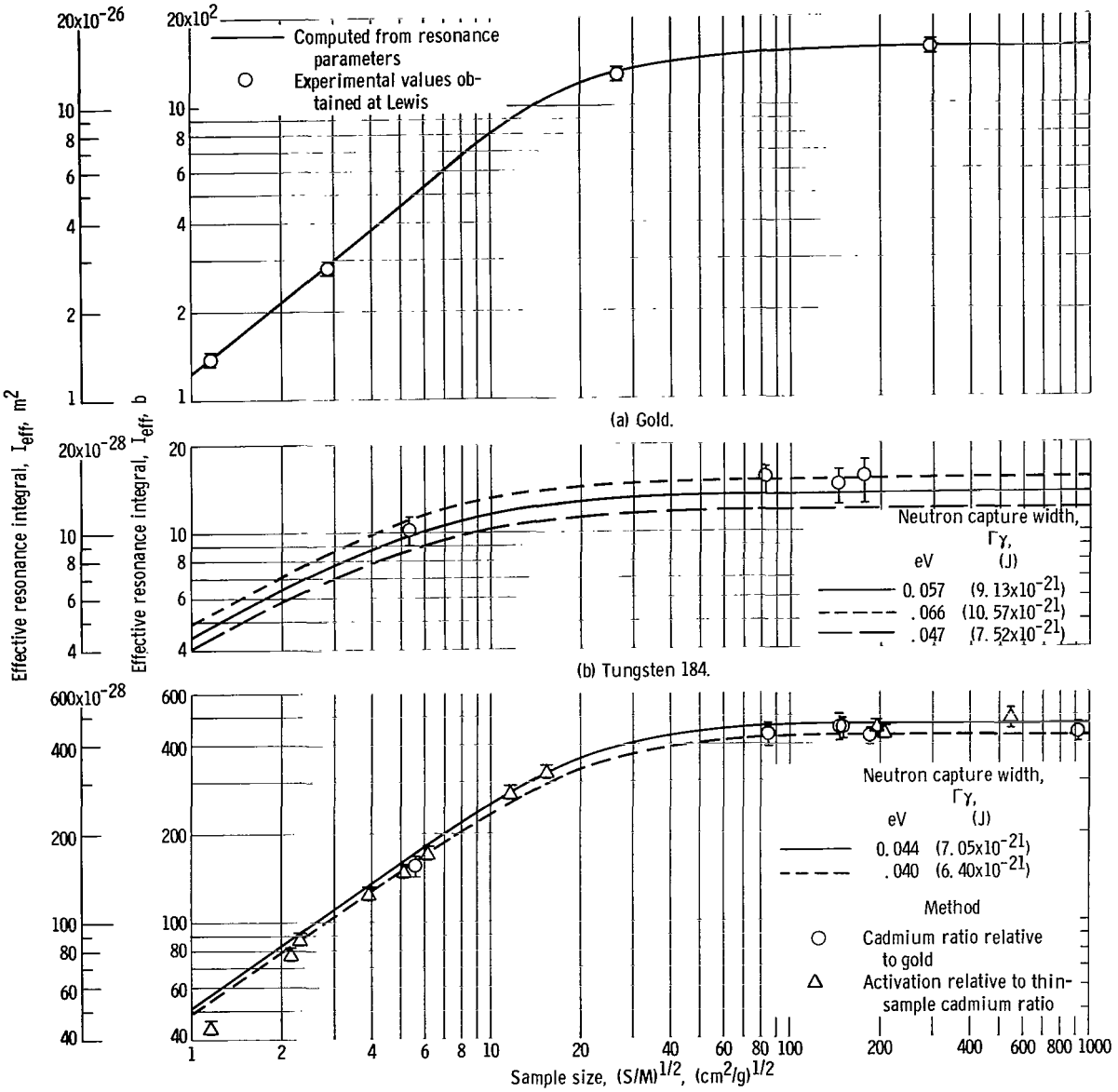

Figure 4. - Effective resonance integral referred to cadmium cutoff energy of 0.5 electron volt (8.0×10^{-20} J). Values include 1/v contribution.

"... aeronautical and space activities of the United States shall be conducted so as to contribute . . . to the expansion of human knowledge of phenomena in the atmosphere and space. The Administration shall provide for the widest practicable and appropriate dissemination of information concerning its activities and the results thereof."

—NATIONAL AERONAUTICS AND SPACE ACT OF 1958

NASA SCIENTIFIC AND TECHNICAL PUBLICATIONS

TECHNICAL REPORTS: Scientific and technical information considered important, complete, and a lasting contribution to existing knowledge.

TECHNICAL NOTES: Information less broad in scope but nevertheless of importance as a contribution to existing knowledge.

TECHNICAL MEMORANDUMS: Information receiving limited distribution because of preliminary data, security classification, or other reasons.

CONTRACTOR REPORTS: Scientific and technical information generated under a NASA contract or grant and considered an important contribution to existing knowledge.

TECHNICAL TRANSLATIONS: Information published in a foreign language considered to merit NASA distribution in English.

SPECIAL PUBLICATIONS: Information derived from or of value to NASA activities. Publications include conference proceedings, monographs, data compilations, handbooks, sourcebooks, and special bibliographies.

TECHNOLOGY UTILIZATION PUBLICATIONS: Information on technology used by NASA that may be of particular interest in commercial and other non-aerospace applications. Publications include Tech Briefs, Technology Utilization Reports and Notes, and Technology Surveys.

Details on the availability of these publications may be obtained from:

SCIENTIFIC AND TECHNICAL INFORMATION DIVISION

NATIONAL AERONAUTICS AND SPACE ADMINISTRATION

Washington, D.C. 20546